



ELSEVIER

Available online at [www.sciencedirect.com](http://www.sciencedirect.com)

SCIENCE @ DIRECT®

Ecological Modelling xxx (2005) xxx–xxx

---



---

**ECOLOGICAL  
MODELLING**


---



---

[www.elsevier.com/locate/ecolmodel](http://www.elsevier.com/locate/ecolmodel)

# Analysis and nonlinear modeling of the mound-building ant *Formica lugubris* spatial multi-scale dynamic in a larch-tree stand of the southern French Alps

Gérard Boudjema<sup>a,\*</sup>, Guy Lempérière<sup>b</sup>, Magali Deschamps-Cottin<sup>c</sup>,  
David George Molland<sup>b</sup>

<sup>a</sup> *Projet IS2/MISTIS, INRIA-Rhone-Alpes 655, av. de l'Europe, 38334 Montbonnot, France*

<sup>b</sup> *Laboratoire de Biologie des Populations d'Altitude, UMR CNRS 5553, Université Joseph Fourier, BP53-F 38041 Grenoble Cedex 09, France*

<sup>c</sup> *Laboratoire de Systématique Evolutive, UPRES Biodiversité, Université de Provence, 13331 Marseille Cedex 03, France*

Received 2 March 2004; received in revised form 22 February 2005; accepted 28 March 2005

---

## Abstract

Determinism in the evolution of a mound-building ant *Formica lugubris* (Hymenoptera:Formicidae) colony and the impact of environmental perturbations were analyzed using several methods. Variation in dome volume of ant-hills and their activity were followed in a larch forest of the southern French Alps for 8 consecutive years. The dynamic of domes was graphically visualized, and the deterministic component of variations was assessed using linear and nonlinear models (neural networks) in the context of auto-regressive and spatial multi-scale dependences hypothesis. An analysis of residuals was carried out (errors from the best global model) and unpredictable data were located in perturbed areas (forest clearings and wind-throws).

The dynamic of ant colony in the stand was simulated constructing a web of interacting neural net models. Evolution of virtual ant-hills was in accordance with real observed dynamic. The study revealed a very active dynamical system resulting from ants self-organizing in dome construction and confirmed that silvicultural practices can have a negative impact on ant colonies.

© 2005 Published by Elsevier B.V.

**Keywords:** Ants; Bioindicator; Forest ecosystem; *Formica lugubris*; Larch-tree stand; Neural network; Multi-scale dynamic; Spatial dynamic; Stepwise multi-linear regression model; Nonlinear coupled map lattice

## 1. Introduction

The genus *Formica* (Hymenoptera:Formicidae) has an holarctic distribution and includes a large number

of polygynous and omnivorous species (Hölldobler and Wilson, 1990). If the genus *Formica* is commonly associated with cold and wet areas, the more specific *Formica rufa* group of species is associated with forest mountain ecosystems (Della Santa, 1995). According to the most recent taxonomic revisions (Betrem, 1960; Kutter, 1977), the eight species that make up the

\* Corresponding author.

E-mail address: [Gerard.Boudjema@inrialpes.fr](mailto:Gerard.Boudjema@inrialpes.fr) (G. Boudjema).

group are *Formica lugubris* (Zett.), *Formica polyctena* (Först.), *Formica rufa* (L.), *Formica cordieri* (Tetz.), *Formica nigricans* (Em.), *Formica aquilonia* (Yarr.), *Formica uralensis* (Ruzs.), *Formica truncorum* (F.). These species are morphologically and biologically very similar and their identification can be rather confusing (Kannowski and Johnson, 1969). Both qualitative and quantitative studies on the *F. rufa* group have already been carried out in various mountain forest ecosystems of the French Pyrenees and Alps by Torossian and Peponnet (1968), Torossian (1977), Torossian et al. (1979) and Torossian and Roques (1984), in the Italian Alps by Ronchetti (1960) and Pavan (1976), in the Swiss Jura (Gris and Cherix, 1977) and more recently in the Vosges area by Nageleisen (1999) and in the southern French Alps (Lempérière et al., 2002).

Because of their ecological interest (predating, cleaning, long term soil changes ...) in those ecosystems, several species of the *Formica* group were protected in Germany, Switzerland, Italy and Austria. In France Torossian et al. (1984) proposed several parameters of ant colonies such as the volume of active (“biovolume”) and deserted (“necrovolume”) domes, as key factors for the assessment of ecological balance of mountain forest ecosystems.

Our more recent study took place in a general program Ecofor on “Biodiversity and Sylviculture” (French Ministry of the Environment) and we proposed to investigate and analyze the relationships between biovolume and necrovolume over a long time scale in a forest stand partially perturbed by clearing and storm with the aim to define guidelines for sustainable forest harvesting.

A previous empirical analysis of data led us to investigate the dynamic of the system itself before dealing with questions of impact of human and natural disturbances. For this task, we used linear and nonlinear modeling which led us to construct a nonlinear coupled map lattice model of the interacting dome web in the studied forest stand. This final model seemed to confirm an important multi-scale deterministic self-organization in the fast dynamic of domes of the stand. Interesting results appeared along the modeling, about possible impacts of perturbations. The possibility to use volume variations as bioindicator of the functioning of mountain forest ecosystems was also discussed.

## 2. Material and methods

The study site was located in a larch stand (no. 66) of *Larix decidua* Mill. at the Matacharre pass (Montmaur, Hautes-Alpes, 44°35'32" Lat M, 5°55'18" long E, slope 18%, orientation ENE). The age of the larch stand was estimated to be 90 years and an average number of 600 trees per ha was recorded.

A study plot of 1 ha was regularly assessed between 1991 and 1998 in order to indirectly follow the fluctuations of *F. lugubris* colonies. The average elevation of the plot was around 1660 m; the plot belong to a set of forest blocks that have been used for the control of soil erosion (RTM: “Restauration des Terrains en Montagne”) using specific reforestation techniques and a choice of adapted tree species. The surface of the plot was entirely covered with ground vegetation.

The ant domes were mapped in each plot using quadrats of 10 m × 10 m. Each dome was precisely located.

Each dome was labeled and described as active, damaged or deserted, and the shape of the domes was recorded as flat, medium or high. Several measures were carried out on each dome. The volume was estimated using the following formula:

$$V = \frac{2}{3} \prod \frac{D}{2} \frac{d}{2} h$$

with:  $\prod = 3.14116D$ , large diameter in metres ( $\pm 0.05$  m);  $d$ , small diameter in metres ( $\pm 0.05$  m);  $h$ , height (calculated as the mean value of  $h_{\max}$  and  $h_{\min}$ ) in metres ( $\pm 0.05$  m).

The “pseudobiovolume” was estimated as the total volume of the domes on the study plots in cubic metre. The “biovolume” was limited to the total volume of active domes, and the “necrovolume” to the total volume of deserted domes, in cubic metre. The activity of the domes was estimated by regular assessments and the evolution and fluctuations of the volumes were followed together in detail over a period of 8 years (except for year 1991, only the total biovolume and necrovolume were collected).

The measures of volumes did not take into account the endogenous part of the nest, which was difficult to estimate by a noninvasive sampling. It was the reason why we used the superficial volume of the dome defined as “the dome” which only gave partial information on the activity of the total colony.

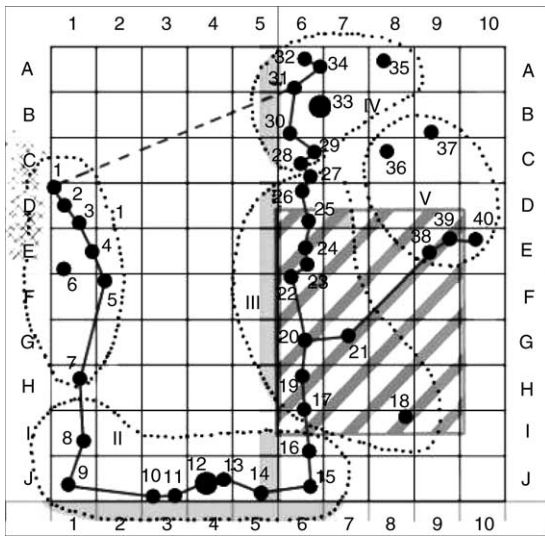


Fig. 1. Map of forest block. Solid lines are the observed main stable ant tracks linking domes (dashed line is a track observed only for the last year of the study). Dashed green zone is the area where clearing was performed during autumn 1991 and gray bands are forest tracks and fire cut-off. Roman numerals indicate the locations of clusters defined in Fig. 4 small dots are arbitrary boundaries of clusters. The set of “xxx” shows 1995 wind-throws location.

A map of the forest block is presented in Fig. 1; lines are the main stable observed ant tracks linking domes (dashed line is a track observed only for the last year of the study), several tests of tolerance acceptance of individuals from different domes transferred in neighboring domes were done to verify the integrity of the cooperon. Hatched zone is the place where clearing was done during 1991 autumn and gray bands are forest tracks and fire cut-off.

Forty different ant-hills locations (reported on the graph) have been observed during the study. It was important to notice that even if a dome disappeared, a new dome could appear at the same place several years later.

**3. Mathematical and statistical analysis**

*3.1. Biovolume and necrovolume*

Correlations between the total volume of active (“biovolume”) and deserted (“necrovolume”) domes in forest block were tested. Neither quantitative nor qualitative (Pearson test, and Spearman rank correlation test,

see Scherrer, 1984) revealed significant links between these two variables.

*3.2. Domes evolutions and volume transfers*

Domes sizes were plotted (with circle diameters proportional to cubic root of domes sizes) and their activities in the field for each year (actives domes in dark, deserted in light gray) in order to visualize details of dynamic transfers (see Fig. 2). Then, to see more clearly aspects of domes dynamic, we computed, according to simple way approach, how the balance could be realized from year to year, obtaining localization of increasing dome and potential locations of their sources. Our assumption was that biovolume moves between closest domes which are very often linked with stable tracks. In our algorithm, positive domes variations were filled with nearest negative domes variations (or the opposite), beginning with the biggest ones in absolute values. While the balance between domes was not set to zero the process was re-launched looking for the next closest neighbors with opposite variations. Each time, computed links were stored and when finished we mapped the transfers of pseudobiovolume from domes to domes, year to year, in the forest block (see Fig. 3).

Visual analysis of Figs. 2 and 3 showed that domes sizes and activities vary a lot each year and also probably during the year. So, some deserted domes have grown up between measures. This implies that an inactive dome can become active and can be deserted the same year. It also seems to appear that multi-scale exchanges occur between close domes, and between dome clusters.

*3.3. Clusters identification and volume transfers between clusters*

The purpose of the following approach was to highlight where stable very active and few active zones were to define clusters boundaries.

The method described as below, pointed out patches with large filling and emptying rates. High active zones remaining the same along years, the graph (Fig. 4) showed separated smoothed peaks and hollows.

As tracks linking domes and their positions in the field were mapped, it was possible to consider that the 40 domes were laid and connected approximately on a line (“track-line”), almost with a ring-topology (thus

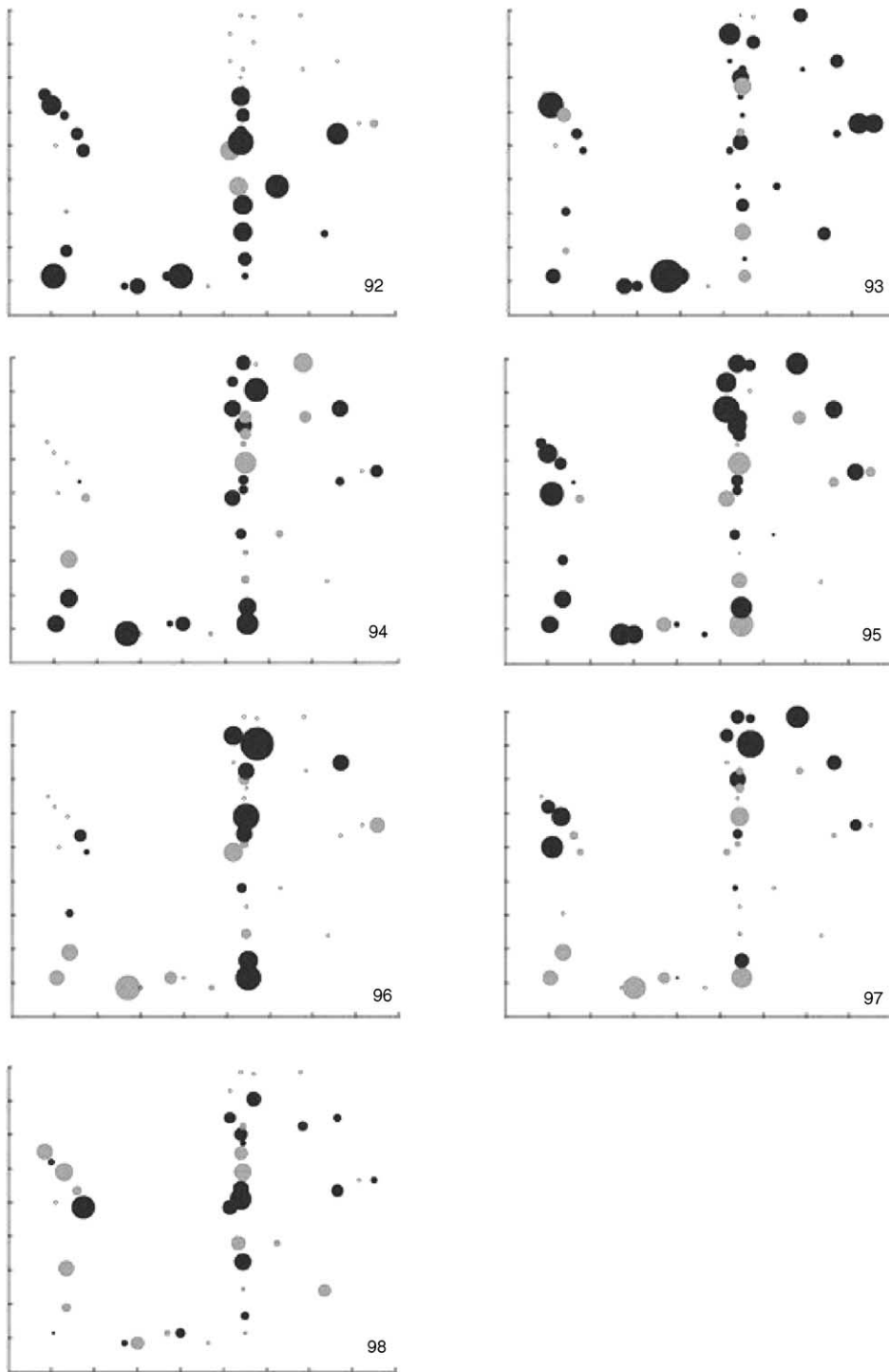


Fig. 2. In the field variation of size and activity of domes in the forest block 66, from year 1992 to year 1998. Diameters were in cubic root of volume. Dark: active domes; light gray: deserted domes.

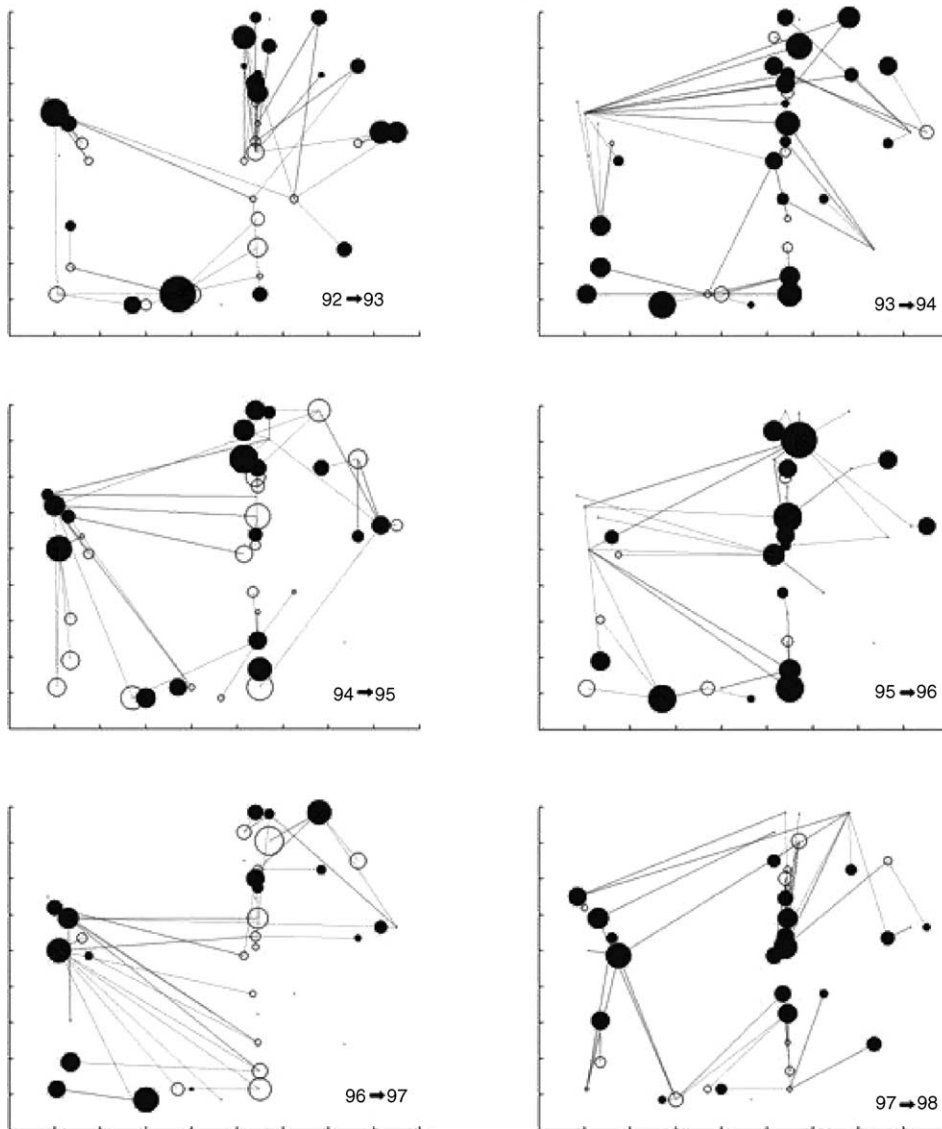


Fig. 3. Location of positive transfers of pseudobiovolume and links of their closest possible sources (dark: increasing domes; white: emptying domes). The assumption to compute these graphs was that biovolumes move between closest domes which were very often linked with stable tracks (for details about the computing see Section 3.2).

191 the dome-space became one-dimensional). Working  
 192 in the “track-line” space, “moving-average windows”  
 193 (MA) at different scales  $j$  of  $|\Delta P_{t,j,i}|$  were computed,  
 194  $P$  being the Pseudobiovolume,  $\Delta P_{t,j,i} = P_{t+1,j,i} - P_{t,j,k}$   
 195 the difference of volume between the years  $t+1$ ,  $t$  at a  
 196 neighborhood level  $j$ , centered on the dome  $i$ . Absolute  
 197 values of  $\Delta P$  were summed on  $t$  and  $j$  for each  $i$ .

Domes laid on the “track-line” in the order of numeration chosen in Fig. 1 were considered and the MA at each scale-level was used as follows:

- first level,  $j=1$ : one dome, the reference dome  $i$ ;
- second level,  $j=2$ : three domes, dome  $i$  and its two neighbors  $[i-1, i+1]$ ;

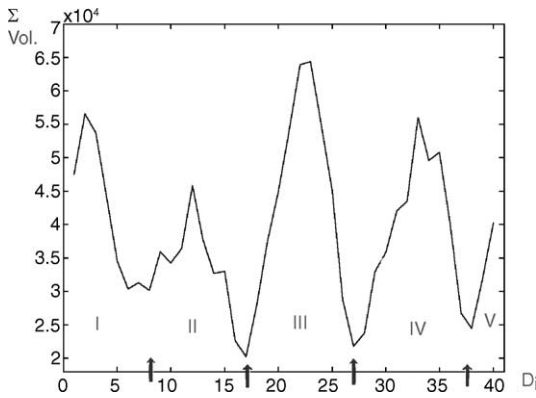


Fig. 4. Global intensity of pseudobiovolumes variation along the “track-line”. Domes ( $D_i$ ) were numbered according to their position on the almost circular track-line (see Fig. 1 and “multi-scale moving-average windows” ( $\Sigma Vol.$ ) were sum on time for each dome (see Section 3.3 for more details). We defined hollows as clusters’ edges (dark arrows). The clusters (I . . . V) corresponded to patches with large filling and emptying rates in their center. High active zones remaining the same along years.

- third level,  $j=3$ : five domes, dome  $i$  and its four neighbors  $[i - 2, i + 2]$ ;
- and so on . . .

We summed on  $j = 1, \dots, 4$  and  $t = 1, \dots, 6$  the value being plotted for each dome  $i = 1, \dots, 40$ . Clusters boundaries were defined where domes showing lowest values between peaks (arrows, Fig. 4).

Operate sum on several scales avoided us to choose a precise working scale and amplified information about activity.

Five clusters (I, II, III, IV, V) were determined, (see Fig. 4, and spots on Fig. 1).

The main observed transfers between these clusters were:

- during 1992 the cluster C-IV was empty (domes have been seen in this area in 1991), the cluster C-III (located in the perturbed area) began to decrease, filling C-IV;
- during 1993–1994, C-I decreased dramatically, C-IV continued to grow and C-III to empty;
- during 1994–1995, C-III, C-IV and C-II fill C-I anew;
- during 1995–1996 the central zone of C-III was completely empty, C-I was empty again;
- during 1996–1997, C-I was filled with transfers from C-IV which showed an important decline;

- during 1997–1998, the pseudobiovolume was concentrated in the center of the stand, C-III was slightly re-colonized.

Each year, local exchanges between close neighbors were also visible, especially in C-II.

### 3.4. Dome size distribution analysis

The dome size distribution (for all years, in block 66) was analyzed using the “Extreme” software developed by IS2 team at INRIA-Rhones-Alpes for extreme events analysis ([www.inrialpes.fr/is2/](http://www.inrialpes.fr/is2/)).

Different models were tested, an exponential law was selected:

$$f(D) = \exp\left(\frac{D^{0.8728}}{226.96}\right)$$

In Fig. 8, we could see that two domes had extreme values superior to  $4 \text{ m}^3$  the probability computed for the exponential law to observe a dome of this size being close to  $1/10000$ .

The first dome (no. 12, 1993) was located in the cluster C-II and the second one (no. 33, 1996) in the cluster C-IV. These two domes seemed to have grown up abnormally, after the clearing for C-III, 1991, and after the wind-throw (touching the cluster C-I during 1995) for the second.

The presence of such very large domes in this forest seemed to be an indicator of environmental perturbations.

### 3.5. Linear modeling using stepwise multiple regression method

According to observations we wanted to test if it was possible to model domes dynamics in a deterministic way, taking into account of multi-scale information. We analyzed data with an explorative method, using Stepwise Multiple Linear Regression (SMLR) method (Draper and Smith, 1981; Scherrer, 1984) to select significant variables amongst a set of potential explicative variables.

In the stepwise multiple linear regression the model was constructed step-by-step. In the first step, the linear model with the more correlated significant variable was computed, then, correlations between residuals and next variables were tested anew with a Fisher test (with

$\alpha = 5\%$ ). The more correlated significant variable was added and the multi-linear model was re-computed, and so on. Previous selected variables partial correlations were tested each time after new models were computed, because two or more new significant variables could contain information brought by an old one (nonindependent variables). This method avoided numerical problems (in matrix inversion) and too much information redundancy in the model variables (selecting significant variables without or few correlations).

This kind of model can be extended with some nonlinear transforms of variables (such as polynomial and logarithmic transforms).

A basic multi-linear model for  $k$  explicative variables gave:

$$Y = a_1 X_1 + a_2 X_2 + \dots + a_k X_k + b$$

with nonlinear transforms using one variable ( $1^\circ$ – $3^\circ$  polynomial transforms in the following example):

$$Y = a'_1 X_1 + a'_2 X_1^2 + a'_3 X_1^3 + \dots + b'$$

A year per year analysis and all years together analysis were carried out. Potential variables to explain variations of a dome  $d_i$  in year  $t$ , were following variables (with delays  $j = 1$  and  $2$ ):

- its past volumes ( $d_i(t-j)$ );
- past volumes of its close neighbors domes: 2 and 4 neighbors, ( $N_i(t-j)_2, N_i(t-j)_4$ );
- past volumes of the clusters sorted according to their distance from the considered dome ( $C_i(t-j)_0, C_i(t-j)_1, C_i(t-j)_2, C_i(t-j)_3, C_i(t-j)_4$ ),  $C_0$  being the cluster including the considered dome;
- logarithmic and  $1^\circ$ – $5^\circ$  polynomial transforms of all these variables.

Results of Stepwise Regressions including natural variables and nonlinear transforms are presented in Table 1.

Each year a model was fitted significantly on data, but each model was different and their ability to ex-

plain data variability very contrasted, ranging from  $R^2 = 0.128$  for 1994 to  $R^2 = 0.86$  for 1997. A global model using all years data, including 2-year delayed dome volume, close neighbors and second closer cluster information of the last year showed a  $R^2 = 0.11$ .

Variability in the selected variables could be explained with redundancies between them, and  $R^2$  variability could result from importance of nonlinear effects and/or external perturbations (like the 1992 cut-off, or the 1995 storm).

### 3.6. Neural network modeling

Once the main explicative variables were selected with SMLR, we modeled global data with neural net (NN) powerful nonlinear method to assess more accurately the deterministic part of dome variations, including possible interactions between variables.

Neural net learning is a very efficient method to fit nonlinear maps. It has been demonstrated that the sum of  $u$ -sigmoidal (or logistic) functions (with  $u$  large enough), could approximate all kinds of continuous maps (Hornik et al., 1989). The parameter sets ( $a_i, b_j$ ) of such functions were obtained here by the conjugate gradients method. A one-hidden layer network with  $u = 8$  neurons was used in this study. (see Anderson and Rosenfeld, 1988; Hertz et al., 1991, for more information on the NN modeling).

For  $k$  explicative variables and  $u$  neurons we have the following model:

$$Y = a_0 + \sum_{i=1}^{i=u} \frac{a_i}{1 + \exp(b_{(i-1)(k+1)} + b_{(i-1)(k+1)+1} X_1 + \dots + b_{(i-1)(k+1)+k} X_k)}$$

The number of neurons was chosen after several trials (NN architectures with 4–12 neurons), 8 being the number where the sum of least squares mean (on 20 models randomly initialised for each architecture tested) began to flatten. This meant that the main

Table 1

$d_i(t)$  Modeling with stepwise linear regression, selected variables and values of multiple regression coefficients were presented here for each year and all years

$d_i(t) = f(\dots)$	94	95	96	97	98	All years
Selected variables	$C_i(t-1)_2$	$d_i(t-1)$	$d_i(t-2)$	$d_i(t-1), d_i(t-2), N_i(t-1)_2$	$C_i(t-1)_1$	$d_i(t-2), N_i(t-1)_2, C_i(t-1)_2$
$R^2$ (linear or nonlinear)	0.128	0.218	0.722	0.86	0.377	0.110

Table 2  
Correlation coefficient between the selected neural network predictions and raw data

Neural network $d_i(t) = F(\dots)$	All years
Input variables	$d_i(t-1), d_i(t-2), N_i(t-1)_2,$ $C_i(t-1)_1, C_i(t-1)_2$
Nonlinear $R^2$	0.745

341 information of data was captured with such a network.  
 342 A more precise model selection (see Moody, 1994  
 343 for a review of NN architecture selection) would be  
 344 generally to preferably choose the NN architecture  
 345 (and also possibly to select explicative variables)  
 346 because some risks such as over-fitting and lack of  
 347 generalization of model can sometime occur. But in  
 348 the context of sigmoidal basis-functions use, aberrant  
 349 models due to over-fitting were very improbable and  
 350 generalization properties can be improved using larger  
 351 networks than needed (Lawrence et al., 1997).

352 Analyzing all years data and using the set of five raw  
 353 variables selected with SMLR models as inputs, we obtained  
 354 several NN models from random initializations  
 355 of learning procedure showing similar properties and  
 356 results (results presented, Table 2, and residuals Fig. 5,  
 357 were from the model which provided the closest histogram  
 358 of dome volume distribution, Fig. 6, during for-

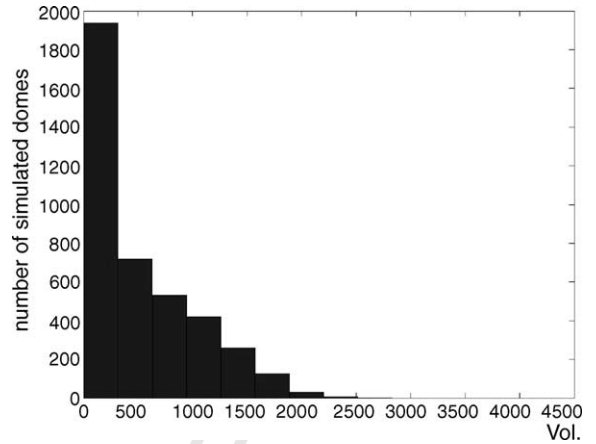


Fig. 6. Histogram: simulated dome volumes distribution. The model presented (Fig. 9 mimicked well real data behavior and features. One can compare this histogram to histogram of Fig. 8.

359 est block-simulation, see Section 3.7, compared to the  
 360 real data observed distribution, Fig. 8).

361 Looking residuals (differences between data and  
 362 model predictions) of the NN model Fig. 5 we saw  
 363 clearly that some data were well explained ( $R^2 = 0.745$ ,  
 364 only 0.11 with SMLR), with residuals close to zero  
 365 (about 50% of the data) and some were surprisingly  
 366 distributed along a straight line with a 45° slope. Those  
 367 residuals were exactly proportional to the data to predict,  
 368 meaning that NN model fitted dynamic of this  
 369 subset of dome like a random process where the best  
 370 possible forecasts were a constant value.

371 When divided in two separated groups (respectively,  
 372 102 and 98 domes) containing well predicted data, the  
 373 wrong ones, according to highness of absolute values of  
 374 their residuals, were visualized on Fig. 7 (X-axis: number  
 375 of mount-building in the field as presented in Fig. 1;

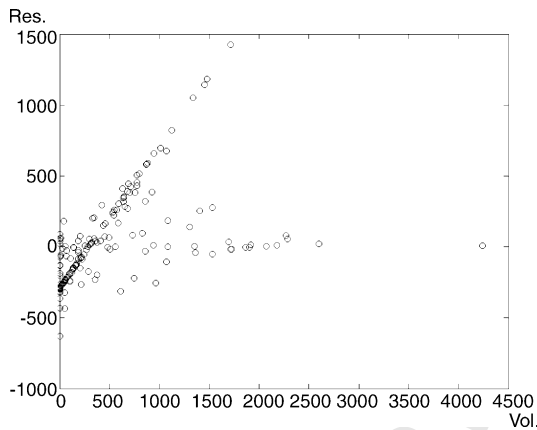


Fig. 5. Plotting of neural network modeling residuals. X-axis: dome volumes; Y-axis: residuals (differences between predictions of the model and raw data). The neural net fail to predict dome volumes lying on the straight line (the value predicted is constant for these domes). It appeared that these badly predicted domes were linked to perturbed zones (see Fig. 7).

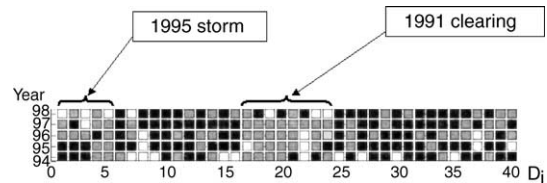


Fig. 7. Domes and their predictability with the neural net model from year 1994 to 1998. Black: well predicted; gray: emptying badly predicted; white: increasing badly predicted. Major densities of badly predicted dome volumes (white and gray) were related to perturbed zones (1991 clearing and 1995 storm).

376 Y-axis: year; Z-axis: mount-building size) the data with  
 377 colors associated to their predictability with the first  
 378 NN model (black: well predicted; gray: wrong predic-  
 379 tion, increasing observed; white: wrong prediction, de-  
 380 creasing observed). We could see that about 30% of  
 381 bad predictions were located in a big spot related to the  
 382 area of the 1992 cut-off (domes number 17–24). “Ab-  
 383 normal” increasing observed on domes number 7, 8,  
 384 9, 15, 16, 25, 27 and 30, during 1994, could be linked  
 385 to evacuation of the perturbed area. The dome num-  
 386 ber 13 destroyed by boars during 1996 was also badly  
 387 predicted. During 1996, bad domes 1, 2, 3 were very  
 388 close of the area destroyed by the 1995 storm. The  
 389 other wrong forecasts could be explained by disrupt-  
 390 ing effects of some local or global unknown factor or  
 391 by random components in ants behavior.

### 392 3.7. Simulation of the global dynamic of the forest 393 block

394 The above neural net model fitting provided for a  
 395 “standard” dome, an auto-regressive map predicting  
 396 next year evolution according to spatial multi-scale de-  
 397 pendences. Thus, each dome state at year  $t+1$  could  
 398 be estimated by a nonlinear function of its past and of  
 399 the state of its neighborhood and close dome clusters.  
 400 Then, it was easy to construct an artificial block forest  
 401 connecting each virtual dome together as observed in  
 402 the field.

403 Simulations were done using the last real observed  
 404 data to initialize the web. One hundred iterations were  
 405 presented in Fig. 9. The interactive domes’ behavior  
 406 showed stable chaotic waves which remained in the  
 407 range of real data. The volume distribution (Fig. 6)  
 408 was exponential and very similar to the observed one  
 409 (Fig. 8). In this simulation, one can see clearly some  
 410 shifting zones (corresponding to clusters areas) very ac-  
 411 tive or almost deserted, sometime during several years.  
 412 The alternation at smaller scale (between close domes),  
 413 more difficult to appreciate on this graph, was also re-  
 414 produced.

415 In our model, all domes were assumed to follow  
 416 the same dynamic in a homogeneous environment, a  
 417 more realistic one would include local environmental  
 418 and ecological constrains limiting the maximal vol-  
 419 ume of domes in the field, leading some to remain  
 420 always small and some others to become more often  
 large.

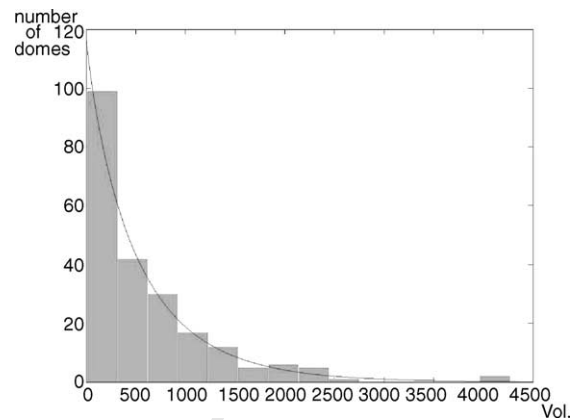


Fig. 8. Histogram: dome volumes distribution; curve: exponential model fitted on data. Observed two domes bigger than  $4\text{ m}^3$  were probably abnormal consequence of clearing and storm damage (the theoretical probability to find such volumes in the field was close to  $1/10,000$ ).

## 421 4. Discussion and conclusion

422 Our modeling strategy was mainly empirical while  
 423 guided by data analysis. At last we constructed a model  
 424 of the expected ants’ forest stand web which was a dis-  
 425 crete time nonlinear coupled map lattice model. This  
 426 kind of model was very interesting to easily model com-  
 427 plex nonlinear systems showing inner synchronization  
 428 or self-organization (Cazelles et al., 1997). Each of the  
 429 40 cells (virtual domes) of the lattice was a neural map  
 430 receiving “past” information about itself and its neigh-  
 431 borhood at multi-scale levels. According to the linear  
 432 and nonlinear analysis (see Sections 3.6 and 3.7) the  
 433 coupling involved three local hierarchical levels (the  
 434 dome, its close neighbors and its close dome clusters).  
 435 Such a model had some characteristics of some re-  
 436 cent models used for landscape studies which included  
 437 spatial auto-correlations (Overmars et al., 2003), hier-  
 438 archical patches (Burnett and Blaschke, 2003), or non-  
 439 linear basis functions modeling (gaussian kernels, in  
 440 Hay et al., 2002). The originality of our model was that  
 441 we worked on an irregular 2D grid of cells which was in  
 442 a sense ‘fractal’ rather than on a continuous landscape  
 443 or regular patches that our linear analysis (SMLR)  
 444 corresponded to estimate multi-scale space–time  
 445 correlations, with selection of the more independent  
 446 variables for nonlinear modeling and that nonlinear ba-  
 447 sis functions we used were applied to the estimation of

448 a “mean” dome dynamical map used to construct the  
449 lattice model. Finally we could run simulations of a dy-  
450 namical recursive model of ants’ activity over the year.

451 In spite of the arbitrariness of our modeling  
452 paradigm, it seemed relevant regarding results of the  
453 NN residual analysis and of the virtual stand simula-  
454 tions (which provided realistic dynamic of dome vol-  
455 umes, without aberrant behaviours and divergences,  
456 though the nonlinear complexity of the lattice).

457 The structure of the ant communities in the two  
458 study plots seemed to be guided by polycalism, i.e.  
459 when the ant population occupied several domes  
460 (Gösswald, 1989). Satellite and mother-colonies were  
461 closely linked and related with visited tracks and  
462 seemed to belong to a suprasocial cooperon (Jaisson,  
463 1993).

464 Several tests of tolerance acceptance of individu-  
465 als from different domes transferred in neighboring  
466 domes were all positive and no sign of aggression  
467 was observed between the members of the different  
468 domes, this observation was in accordance with the re-  
469 sults of our analysis and modeling, showing evidence  
470 for fast biovolume transfers through the whole spotted  
471 area. The analysis of mounds variations over an 8-year-  
472 period showed clearly occurrence of intense and fast  
473 deterministic dynamic. The dynamic appeared space,  
474 scale and time dependent and nonlinear.

475 Dome settlements on the study plots and in the  
476 forest stand seemed to be guided by the conjunction  
477 of favorable micro-environmental factors but their dy-  
478 namic appeared linked with the ecosystem turn-over  
479 (“chemical state” of the building and/or density of prey  
480 and/or building-material availability) and the necrovol-  
481 ume characterized by deserted domes seems more rep-  
482 resentative of the complete exploitation of a zone by  
483 ants than degradation of the ecosystem or of the health  
484 of the colony. Other studies are necessary to understand  
485 the underlying mechanisms (ants auto-organizing pro-  
486 cess according to environmental factors, ...) of such fast  
487 dynamic.

488 The clearings created by the Office National des  
489 Forêts (ONF) and the wind-throw have modified the  
490 forest stand structure and had a significant impact on  
491 the local activity of ant, but no significant correlations  
492 were found linking global variations of pseudobio-  
493 volume, biovolume and necrovolume. The important  
494 decreasing of these volumes observed along the  
495 study must also be considered carefully in nonlinear

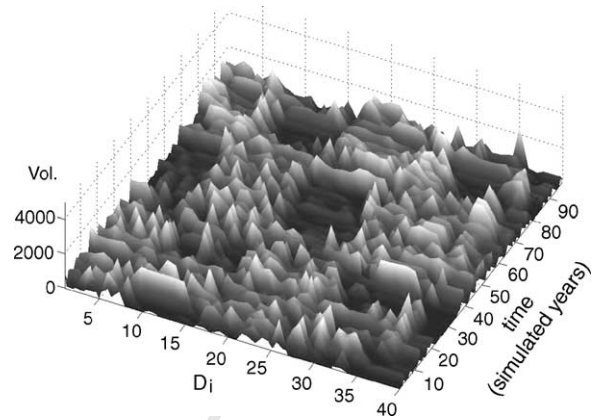


Fig. 9. Hundred years simulation of virtual stand, modeled with neural net web. The 40 domes were modeled, each by its own neural net function, with identical parameters. Interacting neural nets were linked together like observed in the field, varying according to their past and the past states of their neighbors and close clusters (see Section 3.7).

496 context The whole colony did not seem to be at risk  
497 by these local perturbations while the perturbed area  
498 remained limited. Because ants responded quickly by  
499 leaving the nonfavorable zone and concentrating in the  
500 closer clusters, it was possible that the colony could  
501 adapt without problems and that important observed  
502 variations of global pseudobiovolume were natural  
503 fluctuations related to the natural dynamical system  
504 evolution. Our deterministic simulation of a virtual  
505 stand lead to chaotic behaviors looking very erratic  
506 because of the high dimensionality and complexity  
507 of the system. Some year the total pseudobiovolume  
508 could naturally dramatically decrease even without  
509 perturbations. This was why use of volume variations  
510 as bioindicator seemed here unrealistic.

511 Nevertheless, locally, negative effects of clearings  
512 seemed to begin the following year and to persist more  
513 than 6 years after the event in the concerned zone, but  
514 here again, such long deserting of an area could result  
515 from natural nonlinear dynamic (see Fig. 9). In fact, we  
516 concluded to negative effects because nonlinear mod-  
517 els failed to explain the lack of activity in this zone,  
518 and the higher activity around it. Another, possible in-  
519 dicator to highlight perturbation occurrence could be  
520 the presence of extremely large domes ( $>4\text{ m}^3$ , in our  
521 case). But this criterion seemed difficult to generalize  
522 for other stands, because the larch forest appeared to be

a particular biotope, with larch needles being a fragile and a light material easier to carry than pine needles and with a faster decomposition rate.

Other studies are necessary to confirm our work and conclusions. Nevertheless, it is suggested that the practice of clearfelling could be replaced by smaller clearing or by several tree-per-tree thinning operations in order to limit the disturbances on ant colonies. This practice could provide less extreme environments for ant populations, the optimal forest shelter leading to higher biodiversity being between a continuous cover and no cover.

### Uncited references

Evans (1993), Gadau et al. (1996), Rosengren and Pamilo (1983), Torossian and Roques (1979) and Torossian (1984).

### Acknowledgements

This work was followed by a GIP-ECOFOR project of the French Ministry of Environment in the southern French Alps. Many thanks to P. Thomassin, J.L. Rouquet, J.L. Castelle and P. Bellon for their assistance in the field work. We would like to thank K. Day and M. Docherty for providing comments during the preparation of the manuscript.

### References

Anderson, A.J., Rosenfeld, E., 1988. Neurocomputing: Foundation of research. MIT press, Cambridge.

Betrem, J.G., 1960. Über die Systematik der *Formica rufa* Gruppe. Tydschr v Ent. 104 (1/2), 51–81.

Burnett, C., Blaschke, T., 2003. A multi-scale segmentation/object relationship modelling methodology for landscape analysis. Ecol. Modell. 168, 233–249.

Cazelles, B., Boudjema, G., Chau, N.P., 1997. Adaptive synchronization of globally coupled chaotic oscillators using control in noisy environments. Physica D 103, 452–465.

Della Santa, E., 1995. Fourmis de Provence. Faune de Provence (CEEP) 16, 5–38.

Draper, N., Smith, H., 1981. Applied Regression Analysis, second ed. John Wiley and Sons.

Evans, J.D., 1993. Parentage analyses in ant colonies using simple sequence repeat loci. Mol. Ecol. 2, 293–297.

Gadua, J., Heinze, J., Hölldobler, B., Schmid, M., 1996. Population and colony structure of the carpenter ant *Camponatus floridanus*. Mol. Ecol. 5, 785–792.

Gösswald, K., 1989. Die Waldameise: biologische Grundlagen, vol. 1. Ökologie und Verhalten-Aula-Verlag, Wiesbaden, Band, pp. 1–650.

Gris, G., Cherix, D., 1977. Les grandes colonies de fourmis des bois du Jura (groupe *Formica rufa*). Mitt. Schweiz. Entomol. Ges.; Zürich 50, 249–250.

Hay, G.J., Dubé, P., Bouchard, A., Marceau, D.J., 2002. A scale primer for exploring and quantifying complex landscapes. Ecol. Modell. 153, 27–49.

Hertz, J., Krogh, A., Palmer, R.G., 1991. Introduction to the Theory of Neural Computation. Addison-Wesley.

Hölldobler, B., Wilson, H.O., 1990. The Ants. Harvard University Press, Cambridge.

Hornik, K., Stinchcombe, M., White, A., 1989. Multilayer feed-forward networks are universal approximators. Neural Netw. 2, 359–366.

Jaisson, P., 1993. La fourmi et le sociobiologiste. Eds O Jacob, 325 pp.

Kannowski, P.B., Johnson, R.L., 1969. Male patrolling behaviour and sex attraction in ants of the genus *Formica*. Anim. Behav. 17, 425–429, London.

Kutter, H., 1977. Insecta Helvetica Fauna 6. Hymenoptera Formicidae. Schweiz Entomol. Ges.; Zürich, 298.

Lawrence, S., Lee Giles, C., Ah Chung, T., 1997. Lessons in neural networks training: over-fitting may be harder than expected. In: Proceedings of the Fourteenth National Conference on Artificial Intelligence, AAAI-97. AAAI press, Menlo Park, California, pp. 540–545.

Lempérière, G., Bourbon, G., Buray, A., Franchini, S., 2002. Étude des populations de fourmis rouges dans cinq sites du bassin de Gap-Chaudun (Hautes-Alpes). Revue Forestière Française; LIV 5, 419–428.

Moody, J., 1994. Prediction risk and architecture selection for neural networks, Statistics to neural networks and pattern recognition, NATO ASI series F, Springer-Verlag.

Nageleisen, L.M., 1999. Les Fourmis rouges dans le Nord-Est de la France. Revue Forestière Française; LI 4, 487–495.

Overmars, K.P., de Koning, G.H.J., Velkamp, A., 2003. Spatial autocorrelation in multi-scale land use models. Ecol. Modell. 164, 257–270.

Pavan, M., 1976. Utilisation des fourmis du groupe *Formica rufa* pour la défense biologique des forêts. Ministero Agric. I. For., Roma, Collona Verde 39, 417–442.

Ronchetti, G., 1960. Sui trapianti di formiche del “grupo *Formica rufa*” in Italia. Atti Acc. Naz. It. Entom. 8, 218–227.

Rosengren, R., Pamilo, P., 1983. The evolution of polygyny and polydomy in mound-building *Formica* ants. Acta Entomol. Fenn.; Helsinki 42, 65–77.

Scherrer, B., 1984. Biostatistique. Gaëtan Morin ed.

Torossian, C., Peponnet, F., 1968. Rôle de *Formica polyctena* Först dans le maintien des équilibres biologiques forestiers des forêts de feuillus du plateau de Lannemezan. Ann. Epiphyties 19 (1), 97–111.

- 621 Torossian, C., 1977. Etude préliminaire des conséquences ento- 631  
622 mologiques des coupes pratiquées en forêt de Grésigne. Bul- 632  
623 letin de la Société d'Histoire Naturelle de Toulouse 113 (3–4), 633  
624 366–373. 634
- 625 Torossian, C., Roques, L., Alauzet, C., 1979. Rôle des espèces 635  
626 du groupe *Formica rufa* comme indicateur biologique de 636  
627 dégradation du milieu forestier montagnard sous l'action hu- 637  
628 maine. Bulletin SROP, II 3, 265–283. 638
- 629 Torossian, C., Roques, L., 1979. Etude des fourmis du groupe 639  
630 *Formica rufa* des Pyrénées catalanes françaises. Bulletin SROP, 640  
II 3, 243–262.
- Torossian, C., Roques, L., 1984. Les réponses de *Formica lugubris* 631  
Zett à la dégradation anthropique des forêts de l'étage subalpin 632  
français. Bull. Ecol. 14 (1), 77–90. 633
- Torossian, C., Roques, L., Colombel, P., 1984. Dynamique 634  
des populations de la fourmi rousse *Formica lugubris* dans 635  
différents biotopes forestiers montagnards. Acta biol. Mont. IV, 636  
127–148. 637
- Torossian, C., 1984. La protection des fourmis du groupe "Formica 638  
*rufa*" en France. Rapport annuel du Conseil Scientifique Régional 639  
de l'Environnement de Midi-Pyrénées, 33–35. 640

UNCORRECTED PROOF